Hindawi
Journal of Nanomaterials
Volume 2021, Article ID 9556911, 10 pages
https://doi.org/10.1155/2021/9556911

Research Article

Application of Mesoscale Simulation to Explore the pH Response of Eudragit S100 Used as the Novel Colon-Targeted Powder of Pulsatilla Saponin D

Mingcheng Gong,[1] **Zhenhua Chen**,[1] **Liangliang Zhou**,[1] **Feng Gao**,[2] **Jianxin Cheng**,[1] **and Wanqing Zou**[1]

[1]*School of Pharmacy, Jiangxi Science and Technology Normal University, Nanchang 330013, China*
[2]*School of Pharmacy, East China University of Science and Technology, Shanghai 200237, China*

Correspondence should be addressed to Zhenhua Chen; zhenhuachen@jxstnu.edu.cn and Liangliang Zhou; zhoulliang@163.com

Received 22 August 2021; Accepted 10 November 2021; Published 1 December 2021

Academic Editor: Ilaria Fratoddi

As a pH-sensitive nanomaterial, Eudragit S100 has good colon targeting. However, little research has been carried out on its mesoscopic scale. In this paper, the self-assembly behavior of Pulsatilla saponins D (PSD) and Eudragit S100, as well as the loading and release mechanism of PSD, was investigated via computer simulations. The effects of the self-assembly characteristics of PSD and Eudragit S100 in the dry powder state on the drug-carrier ratio were explored by the coarse-grained molecular dynamics (CGMD) method. According to the pH-responsive feature of Eudragit S100, the drug protection under gastric pH conditions and release in colonic pH conditions were simulated through the dissipative particle dynamics (DPD) method, which has provided insights into the microscopic morphological changes in the pH-sensitive drug delivery systems.

1. Introduction

In designing oral colon-targeted drug delivery systems, the dramatic changes in the medical environment are a major challenge, and efforts have been made to investigate new excipients to overcome the difficulties. Results are notable in the field of polymers. Synthetic polymethacrylates can form a thin film coating on the surface of a drug to achieve controlled release. These nanopolymers are synthesised from distinct ratios of dimethylaminoethyl methacrylates, methacrylic acid, and methacrylic acid esters. Among them, Eudragit S100 maintains a nonionised state under acidic conditions and good hydrophobic properties, which help in coating the drug. Under alkaline conditions, it undergoes protonation and dissolves in water, gradually releasing the encapsulated drug [1]. Due to these properties, Eudragit S100 is commonly used in the preparation of colon-targeted formulations.

In recent years, extensive research in the domestic and overseas have been conducted on triterpene saponin, due to its unique anti-inflammatory, anticancer, antibacterial, antiviral, and other medicinal properties [2–5]. Pulsatilla saponin (PS) is a kind of pentacyclic triterpene saponin. Studies conducted by Son et al. [6]. have shown that Pulsatilla saponins D (PSD) acts as an antiangiogenic agent through reducing the expression of HIF-1α and VEGF. It also inhibits the Akt/m TOR signaling pathway to induce apoptosis of colon cancer cells. It is a good candidate for natural products used in the treatment of colon cancer. At present, the treatment of colitis with Pulsatilla is primarily administered orally or by enema. However, the low bioavailability with oral administration and poor patient compliance with enema administration are not ideal. Therefore, based on clinical needs and combined with modern drug delivery technology, Pulsatilla total saponin was transformed into an oral colon-targeted formulation. Not only can the efficacy of the drug be improved but also the portability and ease of administration, thus increasing the willingness of patients to take it [7, 8]. Feng et al. coated Pulsatilla tablets with

pH-sensitive polymer materials, to prepare pH-dependent Pulsatilla colon-targeted tablets for oral administration [9]. Zhao et al. used the central composite design-response surface methodology to optimize the preparation process of the oral Pulsatilla colon-specific release tablets [10]. The coating prescriptions were screened using the total alkaloid in vitro release degree as the index. The results showed that the oral Pulsatilla colon-specific release tablets could better achieve the purpose of colon-specific drug release.

The above method is less affected by food consumption, and the drug absorption rate is uniform. However, it also has disadvantages such as the complicated preparation process, the high requirements of the physical and chemical properties of the material, and troublesome administration in animal experiments. Therefore, in previous work [11], our team introduced the theory of particle design into the preparation process of multidrug colon targeting formulations. We chose the more commonly used mechanochemical method of particle design and have taken advantage of the superfine characteristic of the powder of pH-sensitive EudragitS100 coating material. Pulsatilla extract was made into powder particles with the core-shell structure design, to achieve the purpose of colonic targeting. However, certain restrictions on experimental conditions are not conducive to further exploration of its microstructure and particle distribution. Therefore, we used coarse-grained molecular dynamics (CGMD) and dissipative particle dynamics (DPD) simulations to explore the complex systems, deepen our understanding, and provide valuable guidance for designing new particle powders.

DPD simulation is a calculation method that is more suitable for studying hydrodynamic behavior than the all-atom molecular dynamics method. The calculation concerns the coarse-grained molecular group and is not based on the degree of freedom of internal particles, but rather the motion of the center of mass. Compared with molecular dynamics, the DPD approach has a much larger simulation space and time scale. Wang and Jiang used DPD simulation to investigate the self-assembly behavior of polymeric drug-loaded micelles PEO-PPO-PEO [12]. They also analyzed the drug distribution in the polymeric carriers at different drug-carrier ratios. Wu et al. simulated the formation of four six-arm star-shaped block polymer micelles, the effect of hydrophobic/hydrophilic block ratio on micelle structure, and drug-carrying properties on the morphology of micelles, as well as the effect of the pH-sensitive block ratio on the drug release characteristics [13]. Furthermore, the structural change, the radial distribution function (RDF), and azimuth shift of different pH-sensitive block polymer micelles in weak acidic conditions (pH = 5.0) were compared. The drug release characteristics of the drug-loading micellar system were also analyzed systematically.

2. Modeling and Simulation Methods

2.1. CGMD Theory. CGMD has been used to study the conformation, structure, and self-assembly behavior of polymers, lipids, and amphiphilic macromolecules [14–18]. The MARTINI force field [19, 20] that emerged in 2007 has been developed into a systematic parameterized force field

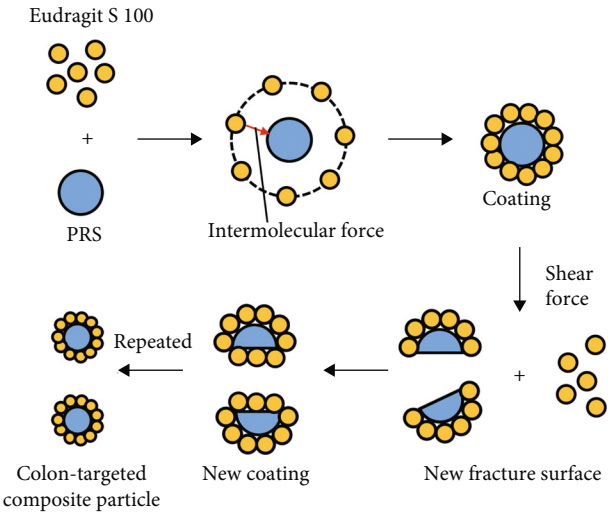

Figure 1: The formation schematic of the particle design powder.

suitable for CGMD simulation. Lennard-Jones (LJ) 12-6 potential energy function has been used to express the van der Waals interaction of particle i and j separated by a distance r_{ij}:

$$V_{\text{Lennard–Jones}}\left(r_{ij}\right) = 4\varepsilon_{ij}\left[\left(\frac{\sigma_{ij}}{r_{ij}}\right)^{12} - \left(\frac{\sigma_{ij}}{r_{ij}}\right)^{6}\right]. \quad (1)$$

In Equation (1), σ_{ij} represents the closest distance between the two particles, and ε_{ij} represents the interaction strength between the two particles. In addition, there is the Coulomb interaction between charged beads, and the potential energy function is expressed as:

$$V_{el} = \frac{q_i q_j}{4\pi\varepsilon_0\varepsilon_{rel} r_{ij}}. \quad (2)$$

In Equation (2), $q_i q_j$ represents two different dotted beads, and the relative dielectric constant ε_{rel} is 15. The following formulas were used to express bond length, bond angle, and dihedral angle potential:

$$V_b = \frac{1}{2}K_b\left(d_{ij} - d_b\right)^2, \quad (3)$$

$$V_a = \frac{1}{2}K_a\left[\cos\left(\varphi_{ijk}\right) - \cos\left(\varphi_a\right)\right]^2, \quad (4)$$

$$V_d = K_d\left[1 + \cos\left(n\psi_{ijkl} - \psi_d\right)\right], \quad (5)$$

where K_b, K_a, K_d, and K_{id} are the force constants. The force constant of resonant potential K_b is 1250 KJmol^{-1} mol^{-2}. For the aliphatic compound, the force constant K_a is 25 KJmol^{-1} rad^{-2}, the balance bond angle ψ_a is 180°. d_b is the balance distance, the angle ψ_{ijkl} is the angle between the plane formed by ijk and jkl, and ψ_d is the balance dihedral angle.

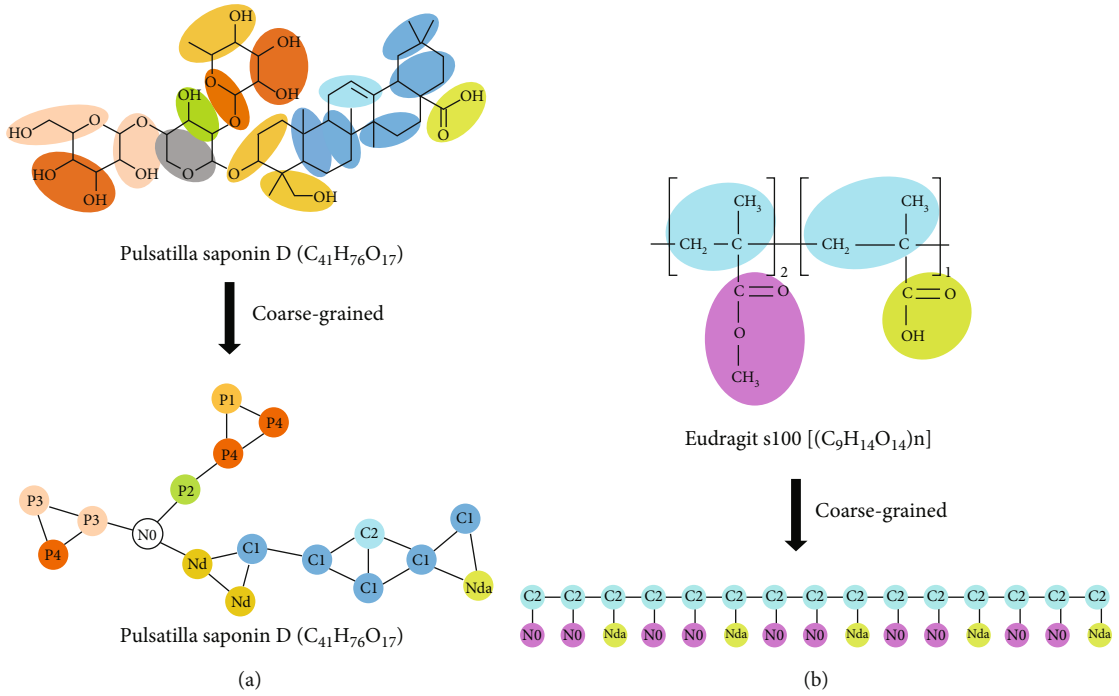

FIGURE 2: Based on the MARTINI force field coarse granulation rules; (a) Pulsatilla saponins D coarse granulation model; (b) Eudragit S100 coarse granulation model.

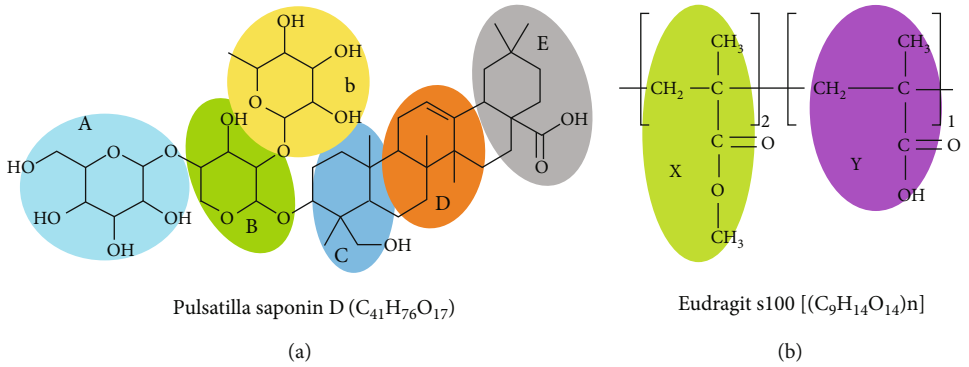

FIGURE 3: DPD coarse granulation model; (a) Pulsatilla saponins D; (b) Eudragit S100.

2.2. DPD Theory. Molecular dynamics is an accurate calculation method at the atomic or molecular scale with some limitations. Due to its unique spatio-temporal scale and satisfactory calculation efficiency, DPD simulation has been widely used [21–24]. It can simulate up to 10^6 atomic systems and dynamic evolution in the ns-μs time scale. In recent years, more and more complex nanocarriers with different structures have been successfully characterized, and the factors affecting nanocarriers have been parameterized. DPD simulations emphasize not only the self-assembly structure of nanocarriers but also their synthesis, preparation, and interaction with biological membranes.

DPD is a mesoscopic simulation method proposed by Hoogerbrugge and Koelman in 1992 [25], to describe the mesoscopic level properties in the formation of polymer nanoparticles. Through the coarse division of molecules and the definition of different beads to simplify the system and reduce the computing performance requirements of the service, the mesoscopic concept builds a bridge between fast molecular dynamics and slow macrothermodynamics. The motion of all beads in the DPD simulation follows Newton's laws of motion:

$$\frac{dr_i}{d_t} = v_i, m_i \frac{dv_i}{d_t} = f_i. \tag{6}$$

In Equation (6), r_i, v_i, m_i, and f_i represent the vector position, speed, mass, and total force received by the bead i, respectively. For a bead, the total force it receives is composed of three parts [26]:

$$f_i = \sum_{j \neq i} \left(F_{ij}^C + F_{ij}^D + F_{ij}^R \right). \tag{7}$$

Table 1: The rejection force parameters in the DPD simulation.

	X	Y	Y-	A	B	C	D	E	b	w
X	25									
Y	25.15	25								
Y-	297.3	—	25							
A	57.6	50.4	916.8	25						
B	54.3	48.1	673.9	25.7	25					
C	37.7	33.7	724.2	30.4	33.1	25				
D	35	31.7	651.1	31.6	34.2	25.1	25			
E	43	38	802.8	27.8	27.1	25.5	25.9	25		
b	53.8	47.2	845.8	25	25.9	29.4	30.4	27.1	25	
w	108	106	17.7	405.9	287.6	301.9	327.1	341.4	371.6	25

$F^C{}_{ij}$, $F^D{}_{ij}$, and $F^R{}_{ij}$ are the conservative force, the dissipative force, and the random force, respectively, and they occur in pairs.

$$F_{ij}^C = -a_{ij}\left(1 - \left|r_{ij}\right|\right)\hat{r}_{ij}, \tag{8}$$

$$F_{ij}^D = \lambda\omega^D\left(r_{ij}\right)\left(\hat{r}_{ij}v_{ij}\right)\hat{r}_{ij}, \tag{9}$$

$$F_{ij}^R = -\sigma\omega^R\left(r_{ij}\right)\theta_{ij}\hat{r}_{ij}. \tag{10}$$

Among them, a_{ij} is the maximum repulsion between particles i and j, $r_{ij} = r_j - r_i$, $\hat{r}_{ij} = r_{ij}/|r_{ij}|$. $\omega^D(r_{ij})$ and $\omega^R(r_{ij})$ are two short-range weight functions, $\theta_{ij}(t)$ is a random variable with compound Gaussian distribution, and there are $\langle\theta_{ij}(t)\rangle = 0$ and $\langle\theta_{ij}(t)\rangle\langle\theta_{kl}(k^l)\rangle = (\delta_{jk}\delta_{jl} + \delta_{il}\delta_{jk})\delta(t - t^{'})$. In order to obtain the interbead rejection parameter a_{ij}, the linear relationship between it and the Flory-Huggins parameter χ is [27]:

$$a_{ij} = a_{ii} + 3.27\chi_{ij}\ (\rho = 3). \tag{11}$$

In Equation (11), ρ is the number density. In this work, ρ is set to 3. Among them, the Flory-Huggins parameter χ can be obtained from the solubility parameter δ obtained by calculating the intermolecular interaction strength and cohesive energy of liquid objects [28, 29]:

$$\chi_{ij} = \frac{V_{\text{mol}}}{RT}\left(\delta_i - \delta_j\right)^2. \tag{12}$$

In Equation (12), V_{mol} is the average molar volume of beads i and j, and R and T are the gas constant and thermodynamic temperature, respectively.

2.3. Coarse-Grained Model and Input Parameters. There is no solvent involved in the preparation process of the particle design powder; it is purely a mixture of solid powders. The formation schematic of the melding is shown in Figure 1. In this study, we adopted the CGMD method to simulate the self-assembly process of the polymer and drug, and then, we used the DPD method to simulate the pH response in the colonic fluid.

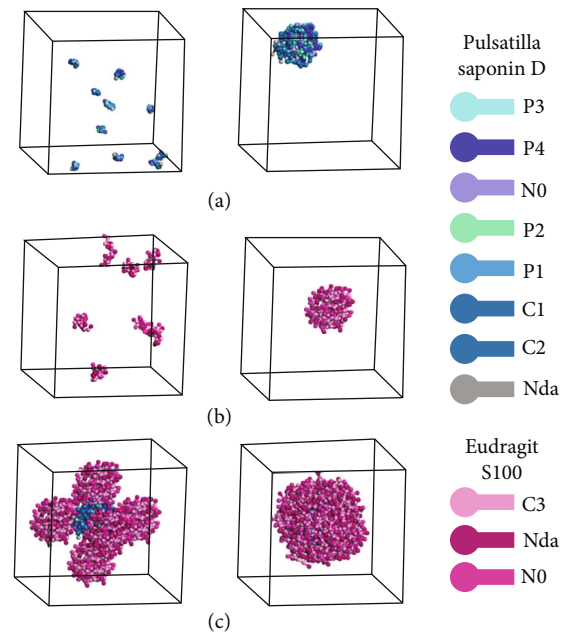

Figure 4: (a) Pulsatilla saponins D forming cluster; (b) Eudragit S100 forming cluster; (c) Pulsatilla saponins D and Eudragit S100 forming cluster.

Since the content of PSD is the highest in the total saponins of Pulsatilla, this simulation is based on the coarse-grained rule of the MARTINI force field [30]. The full-atom structures of PSD and Eudragit S100 were converted into coarse-grained models (see Figure 2). Next, the DPD simulation was carried out. According to the size of the coarse particles, PSD was divided into A, B, b, C, D, and E beads, and Eudragit S100 was divided into X and Y beads. The deprotonation reaction of Y beads under alkaline conditions is defined as the Y^-bead (see Figure 3). Eudragit S100 monomer contains carboxyl group (-COOH); thus, it is not easily decomposed by oral administration in gastric juice. When the drug enters the colon, it is in an alkaline environment. The carboxyl group on Eudragit S100 is deprotonated to be negatively charged (-COO-), and the Y beads become Y^- beads. In addition, three water molecules are considered to be one w bead.

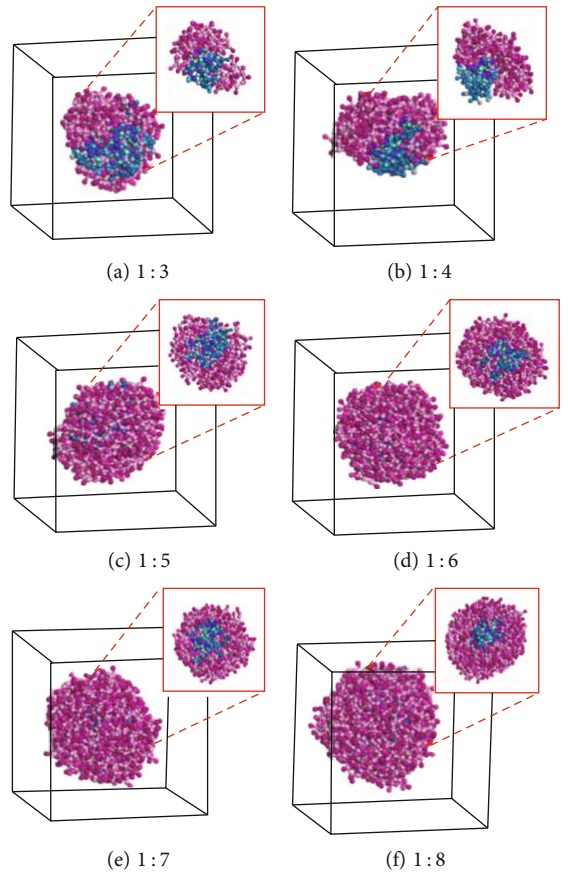

Figure 5: Self-assembled profile of the arrangement of the drug-carrier ratios: 1 : 3, 1 : 4, 1 : 5, 1 : 6, and 1 : 7.

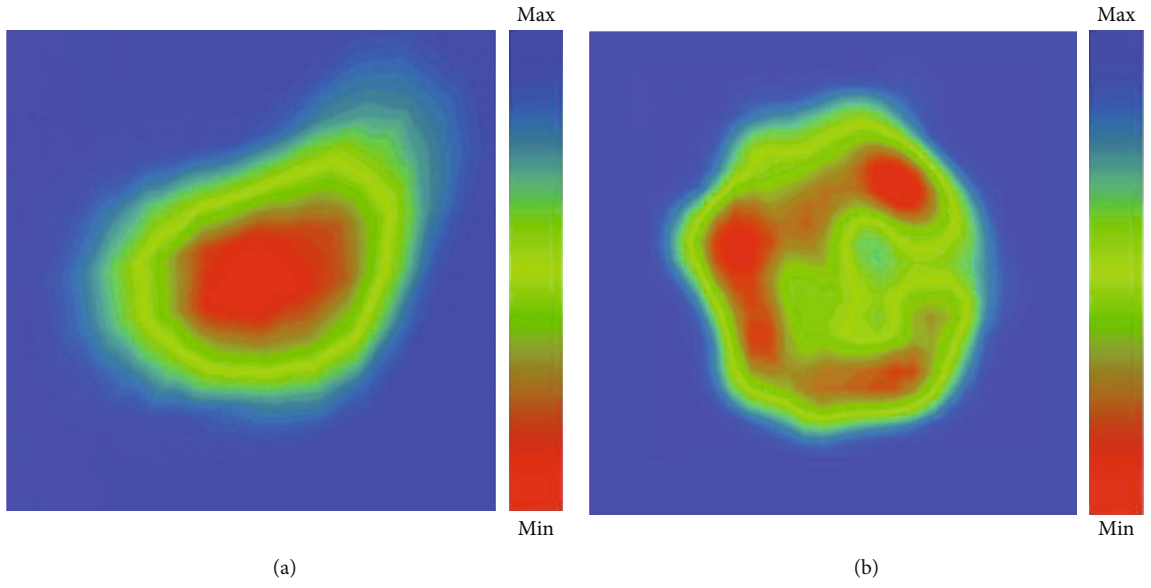

Figure 6: Density field of the drug-carrier ratio is 1 : 6: (a) Pulsatilla saponins D; (b) Eudragit S100.

For this simulation system, using the COMPASS force field in Materials Studio 8.0, which involves the combination of the solubility parameter model and all atomic molecular dynamics (AAMD), the Forcite module was used to calculate the solubility parameter δ of each bead at room temperature (298 K) and obtain the repulsion parameter *aij* between the beads (see Table 1). The smaller the repulsive force parameter between the beads, the better the attractiveness; the larger

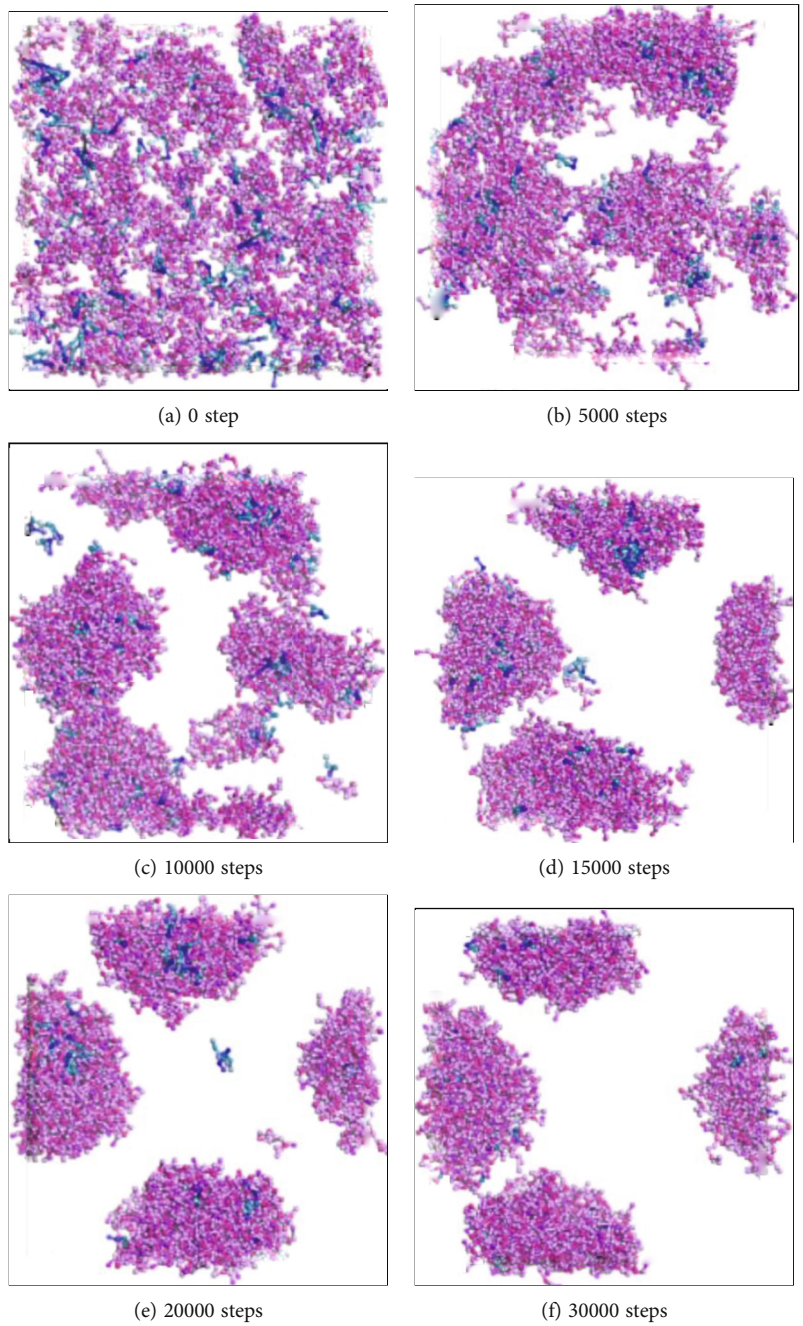

(a) 0 step (b) 5000 steps

(c) 10000 steps (d) 15000 steps

(e) 20000 steps (f) 30000 steps

Figure 7: Change of aggregates with increasing simulation steps.

the repulsive force parameter, the worse the attractiveness. Therefore, it can be seen from the table that the parameters of the repulsive force between the PSD beads and the water beads was too large. This is consistent with the hydrophobic nature of PSD. The repulsive force parameter between Eudragit S100 and water beads was also large, which is in accordance with its hydrophobic nature. Therefore, this coarse-grained model demonstrates the water insolubility of the drug-carrying system.

The size of the CGMD simulation box in this paper is 150 Å × 150 Å × 150 Å. The size of the DPD simulation box is 200 Å × 200 Å × 200 Å. The NVT (the same number of molecules, the same volume, and the same temperature) ensemble was adopted, the three-dimensional periodic boundary conditions were adopted, and the total simulation time was 30,000 steps.

3. Results and Discussion

3.1. Comparison between the Morphology of Simulated Dry Powder Self-Assembly and SEM. In order to reproduce the process of dry mixing as much as possible, PSD and Eudragit S100 beads were randomly dispersed in the boxes to form clusters (see Figure 4). In Figure 4, beads were named with

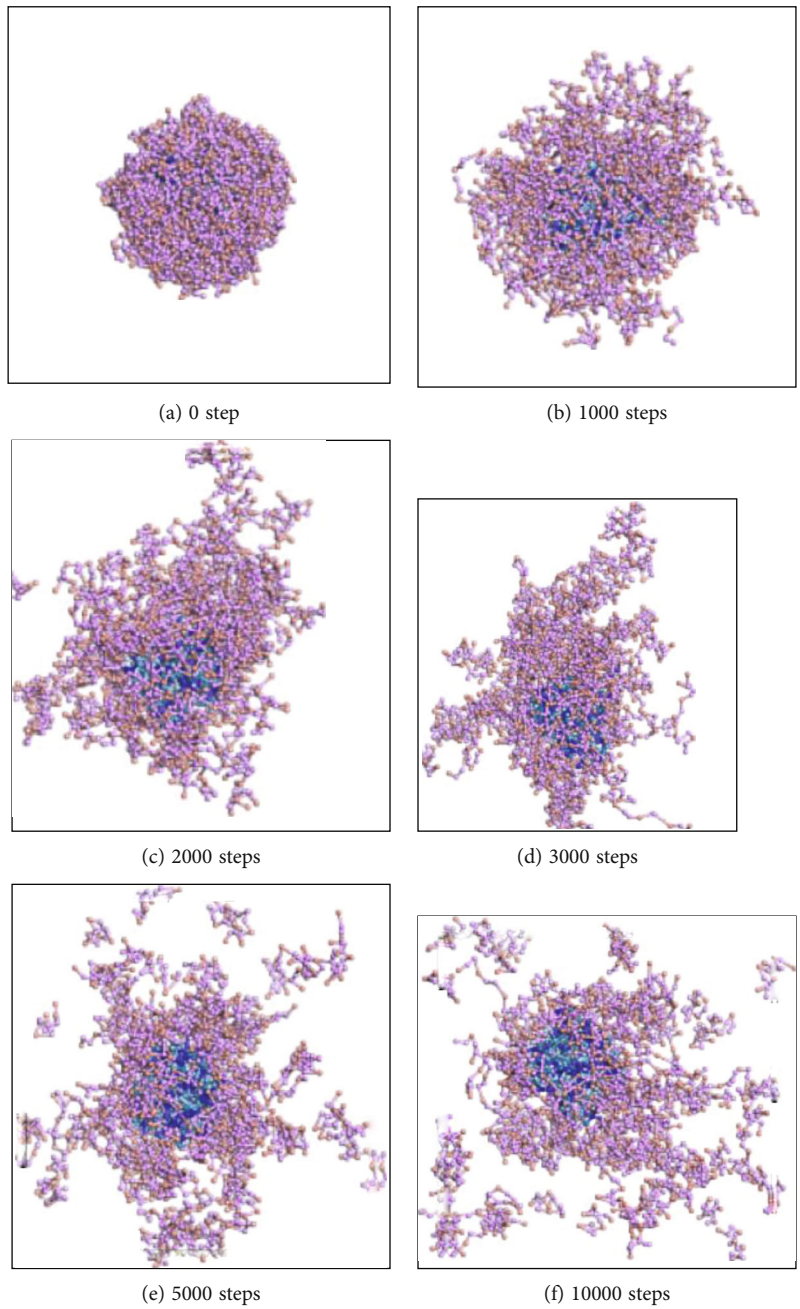

(a) 0 step (b) 1000 steps

(c) 2000 steps (d) 3000 steps

(e) 5000 steps (f) 10000 steps

Figure 8: pH-responsive drug release behavior of the drug system.

the MARTINI forcefield type name. Blue beads and gray beads, such as P3, P4, N0, and more, are PSD beads, and red beads such as C3, Nda, and N0 are Eudragit S100 beads. Then, calculation was performed according to the arrangement of the drug-carrier ratios: 1 : 3, 1 : 4, 1 : 5, 1 : 6, and 1 : 7 (see Figure 5).

The results showed that both PSD and Eudragit S100 dry powder could form clusters, respectively. When mixing the two with a small proportion of Eudragit S100, PSD could not be completely included. The drug was thus quickly released before reaching the target site. When the drug-carrier ratio was 1 : 6, Eudragit S100 and PSD produced a core-shell structure and adhered evenly to it. There was neither excessive drug loading nor too thick coating due to excessive excipients. Taking one bead from both Eudragit S100 and PSD to represent the entire molecule and perform Density Field analysis, it was found that PSD constituted the core of the system (see Figure 6(a)). At the same time, Eudragit S100 formed the shell of the system (see Figure 6(b)). This was consistent with the previous scanning electron microscope (SEM) result of the research team [11]. Previous studies shown that when the drug-carrier ratio was 3 : 7, the rough *P. chinensis* saponins (PRS) were exposed, the drug was included at 3 : 17, and the coating was thicker at 1 : 19.

3.2. Self-Assembly Morphology at pH < 7. Generally, polymers can self-assemble to form nanoparticles in water and form an outer shell while the hydrophobic drugs form an inner core. From the discussion above, it can be concluded that the best condition is when the drug-carrier ratio is 1 : 6. Hence, this ratio was used to simulate the 30000-step DPD in an acidic environment. As shown in Figure 7, the water beads have been hidden for better observation.

At the beginning of the simulation, all the beads were randomly dispersed in water to form a homogeneous solution, and the polymer could be stretched well. As the simulation progressed, the hydrophobic polymer aggregated due to the repelling effect of water and formed the hydrophobic core of the nanoparticle, while the hydrophilic polymer was evenly distributed on the surface, forming small clusters. Due to surface tension, the clusters gradually expanded and merged, then finally formed a complete and compact drug-carrying system with a core-shell structure showing little change in morphology, shape, structure, and size. This indicates that the system was in a relatively stable structure.

3.3. pH-Induced Morphological Evolution of Self-Assembly. The key aspect of the system is to achieve the targeted release in the colon. Therefore, the excipient should release the drug under the condition of colonic pH (pH > 7). The carboxyl groups in bead Y can deprotonate in response to changes in environmental pH, and electrostatic repulsion is dominant. Due to the increase of the repulsive force between the polymer beads and the reduction of the force between the polymer bead and the water bead, the solubility of the polymer is improved, and the effect of releasing it in an alkaline environment is achieved.

The DPD simulation results are shown in Figure 8. When pH < 7, the pH sensitive bead Y is a hydrophobic molecule, and the polymer molecules are self-assembled into a compact shell structure. When the drug enters the colon at pH > 7, it can be clearly seen from the profile that the spherical micelle shape gradually begins to deform. Eudragit S100 polymer no longer tightly wraps around the PSD surface, and the same charged beads repel each other, resulting in considerable stretching between the X and Y beads. After a long simulation time, the self-assembly morphology remains basically unchanged, indicating that the system approaches an equilibrium state. It can be observed that most drug molecules are dispersed outside the micelles, indicating that drug molecules are fully released.

To more accurately reflect the changes of the system before and after protonation and the distribution of beads, the system radial distribution function (RDF) before and after drug release was analyzed (see Figure 9). It can be seen from the figure that under acidic conditions, pH-sensitive segment Y in polymer does not deprotonate, and the aggregate force in the system is greater than the classical repulsion force, so it can be well gathered into the nucleus-shell structure. When pH > 7, Y deprotonation occurs, and electrostatic repulsion force between the Y^- beads began to overcome hydrophobic interaction and gradually spread out, leading to the disintegration of the system.

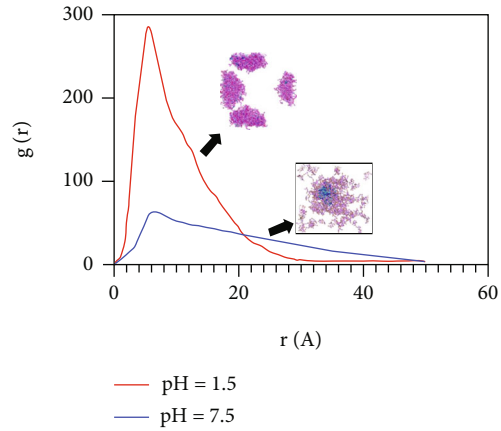

Figure 9: The system RDF before and after drug release.

4. Conclusions

The purpose of this study is to develop a pH-responsive polymer system that can effectively release PSD in the colon. The theory of particle design powder was introduced into the preparation process of multidrug colon-targeted formulations. Commonly used mechanochemical methods in particle design were selected, and using the pH-dependent coating material Eudragit S100 as an ultrafine powder, PRS was made into design powder particles with a shell structure surrounding the core, and the phase behavior of polymer and drug was simulated. First, the CGMD method was used to simulate the optimal ratio between PSD and Eudragit S100, and then, the DPD method was employed to simulate the effect of pH on the morphology of aggregates. When the drug-carrier ratio was different, the assembly effect of the nanoparticles changed, which affected the inclusion and release of the drug. When the drug-carrier ratio was 1 : 6, the best inclusion conditions were achieved. At pH < 7, nanoparticles with normal drug encapsulation by the excipients were obtained. At pH > 7, Eudragit S100 was deprotonated, hydrophilicity was enhanced, and the material was gradually dispersed in water, creating conditions for drug release, which is consistent with the previous research results of our group. In summary, DPD simulation and theoretical analysis can better guide researchers in the design, preparation, and optimization of drug systems.

Data Availability

The data used to support the findings of this study are available from the corresponding author upon request (Zhenhua Chen: zhenhuachen@jxstnu.edu.cn).

Conflicts of Interest

The authors declare no conflicts of interest.

Acknowledgments

The work was supported by the Natural Science Foundation Youth Project (grant number 81703716), grant of Natural

Science Foundation of Jiangxi Province (grant number 20202BABL206151), Youth Talents Project of Jiangxi Science and Technology Normal University (grant number 2017QNBJRC006), and National Undergraduate Training Program for Innovation (grant number 202011318003).

References

[1] S. Guo, G. Wang, T. Wu, F. Bai, J. Xu, and X. Zhang, "Solid dispersion of berberine hydrochloride and Eudragit® S100: formulation, physicochemical characterization and cytotoxicity evaluation," *Journal of Drug Delivery Science and Technology*, vol. 40, pp. 21–27, 2017.

[2] Z. Fang, J. Li, R. Yang, L. Fang, and Y. Zhang, "A review: the triterpenoid saponins and biological activities of Lonicera Linn," *Molecules*, vol. 25, no. 17, p. 3773, 2020.

[3] J.-H. Yu, Z.-P. Yu, Y.-Y. Wang et al., "Triterpenoids and triterpenoid saponins from *Dipsacus asper* and their cytotoxic and antibacterial activities," *Phytochemistry*, vol. 162, pp. 241–249, 2019.

[4] X.-G. Liu, Y.-Q. Sun, J. Bian et al., "Neuroprotective effects of triterpenoid saponins from *Medicago sativa* L. against H_2O_2-induced oxidative stress in SH-SY5Y cells," *Bioorganic Chemistry*, vol. 83, pp. 468–476, 2019.

[5] W. Liu, S. Deng, D. Zhou et al., "3,4-seco-Dammarane triterpenoid saponins with anti-inflammatory activity isolated from the leaves of *Cyclocarya paliurus*," *Journal of Agricultural and Food Chemistry*, vol. 68, no. 7, pp. 2041–2053, 2020.

[6] M. K. Son, K. H. Jung, S.-W. Hong et al., "SB365, _Pulsatilla_ saponin D suppresses the proliferation of human colon cancer cells and induces apoptosis by modulating the AKT/mTOR signalling pathway," *Food Chemistry*, vol. 136, no. 1, pp. 26–33, 2013.

[7] M. Kanamala, W. R. Wilson, M. Yang, B. D. Palmer, and Z. Wu, "Mechanisms and biomaterials in pH-responsive tumour targeted drug delivery: a review," *Biomaterials*, vol. 85, pp. 152–167, 2016.

[8] R. Arévalo-Pérez, C. Maderuelo, and J. M. Lanao, "Recent advances in colon drug delivery systems," *Journal of Controlled Release*, vol. 327, pp. 703–724, 2020.

[9] G. Feng, W. Liu, and Y. Feng, "Preparation and in vitro release evaluation of compound Baitouweng decoction colonic sustained-release tablets," *Journal of GuiZhou University of Traditional Chinese Medicine*, vol. 34, pp. 10–14, 2012.

[10] J. Zhao, X. Kuang, N. Feng, H. Mei, P. Chai, and Y. Zhang, "Preparation process of oral colon-specific delivery tablet of "BaitouwengRecipe."," *Journal of Shanghai University of Traditional Chinese Medicine*, vol. 23, pp. 69–72, 2009.

[11] Z. Chen, Y. Guan, L. Zhou, Y. Xu, M. Yang, and H. Liu, "Preparation and characterization of colon-targeted particles of Pulsatilla chinensis saponins," *Natural Product Communications*, vol. 10, no. 2, p. 1934578X1501000, 2015.

[12] Z. Wang and J. Jiang, "Dissipative particle dynamics simulation on paclitaxel loaded PEO–PPO–PEO block copolymer micelles," *Journal of Nanoscience and Nanotechnology*, vol. 14, no. 3, pp. 2644–2647, 2014.

[13] W. Wu, P. Yi, J. Zhang et al., "4/6-Herto-arm and 4/6-mikto-arm star-shaped block polymeric drug-loaded micelles and their pH-responsive controlled release properties: a dissipative particle dynamics simulation," *Physical Chemistry Chemical Physics*, vol. 21, no. 27, pp. 15222–15232, 2019.

[14] Y. Liu, F. Zhao, J. Dun, X. Qi, and D. Cao, "Lecithin/isopropyl myristate reverse micelles as transdermal insulin carriers: experimental evaluation and molecular dynamics simulation," *Journal of Drug Delivery Science and Technology*, vol. 59, article 101891, 2020.

[15] N. Chiangraeng, V. S. Lee, and P. Nimmanpipug, "Coarse-grained modelling and temperature effect on the morphology of PS-b-PI copolymer," *Polymers*, vol. 11, no. 6, p. 1008, 2019.

[16] H. Sun, W. Yang, R. Chen, and X. Kang, "A coarse-grained water model for mesoscale simulation of clay-water interaction," *Journal of Molecular Liquids*, vol. 318, article 114085, 2020.

[17] F. R. Souza, F. Fornasier, A. S. Carvalho, B. M. Silva, M. C. Lima, and A. S. Pimentel, "Polymer-coated gold nanoparticles and polymeric nanoparticles as nanocarrier of the BP100 antimicrobial peptide through a lung surfactant model," *Journal of Molecular Liquids*, vol. 314, article 113661, 2020.

[18] A. S. Raman, A. Vishnyakov, and Y. C. Chiew, "A coarse-grained model for PCL: conformation, self-assembly of MePEG-b-PCL amphiphilic diblock copolymers," *Molecular Simulation*, vol. 43, no. 2, pp. 92–101, 2017.

[19] S. J. Marrink, A. H. de Vries, and A. E. Mark, "Coarse grained model for semiquantitative lipid simulations," *The Journal of Physical Chemistry. B*, vol. 108, no. 2, pp. 750–760, 2004.

[20] S. J. Marrink, H. J. Risselada, S. Yefimov, D. P. Tieleman, and A. H. de Vries, "The MARTINI force field: coarse grained model for biomolecular simulations," *The Journal of Physical Chemistry. B*, vol. 111, no. 27, pp. 7812–7824, 2007.

[21] W. Min, D. Zhao, X. Quan, D. Sun, L. Li, and J. Zhou, "Computer simulations on the pH-sensitive tri-block copolymer containing zwitterionic sulfobetaine as a novel anti-cancer drug carrier," *Colloids and Surfaces B: Biointerfaces*, vol. 152, pp. 260–268, 2017.

[22] C. Yang, Z. Xue, Y. Liu et al., "Delivery of anticancer drug using pH-sensitive micelles from triblock copolymer MPEG-_b_ -PBAE- _b_ -PLA," *Materials Science and Engineering: C*, vol. 84, pp. 254–262, 2018.

[23] Y. Wang, B. Z. Chen, Y. J. Liu, Z. M. Wu, and X. D. Guo, "Application of mesoscale simulation to explore the aggregate morphology of pH- sensitive nanoparticles used as the oral drug delivery carriers under different conditions," *Colloids and Surfaces B: Biointerfaces*, vol. 151, pp. 280–286, 2017.

[24] L. Shu, F. Fu, Z. Huang, Y. Huang, P. Hu, and X. Pan, "Nanostructure of DiR-loaded solid lipid nanoparticles with potential bioimaging functions," *AAPS PharmSciTech*, vol. 21, no. 8, p. 321, 2020.

[25] P. J. Hoogerbrugge and J. M. V. A. Koelman, "Simulating microscopic hydrodynamic phenomena with dissipative particle dynamics," *Europhysics Letters*, vol. 19, no. 3, pp. 155–160, 1992.

[26] T. Yue, X. Wang, F. Huang, and X. Zhang, "An unusual pathway for the membrane wrapping of rodlike nanoparticles and the orientation-and membrane wrapping-dependent nanoparticle interaction," *Nanoscale*, vol. 5, no. 20, pp. 9888–9896, 2013.

[27] C. Zhong and D. Liu, "Understanding multicompartment micelles using dissipative particle dynamics simulation," *Macromolecular Theory and Simulations*, vol. 16, no. 2, pp. 141–157, 2007.

[28] Z. Luo and J. Jiang, "pH-sensitive drug loading/releasing in amphiphilic copolymer PAE-PEG: integrating molecular dynamics and dissipative particle dynamics simulations," *Journal of Controlled Release*, vol. 162, no. 1, pp. 185–193, 2012.

[29] C. Yang, C. Yuan, W. Liu et al., "DPD studies on mixed micelles self-assembled from MPEG-PDEAEMA and MPEG-PCL for controlled doxorubicin release," *Colloids and Surfaces B: Biointerfaces*, vol. 178, pp. 56–65, 2019.

[30] Z. Chen, S. Liu, Y. Zou et al., "Determination of four saponins in Pulsatillae extract by HPLC," *Journal of Chinese Medicinal Materials*, vol. 39, pp. 352–354, 2016.